2

Modelling of Geological Hazards and Resources

Global Positioning System (GPS) based Geodesy had become capable of yielding sub-cm precision in location by the early 1990s and the possibility of it being used to determine crustal strain rates in India was recognised at C-MMACS in 1993 following the Khillari earthquake. Research at C-MMACS, has since yielded fairly well constrained figures for the velocity of the Indian plate and partitioning of strain from Kanya-Kumari to Ladakh in the trans-Himalaya. Over the years C-MMACS has also taken up the ardous task of setting up GPS stations in remote locations in the country to generate required data base.

Analysis and modelling of GPS data as well as other modelling studies on geophysical processes have generated valuable insight for understanding geological/geophysical processes over the Indian region, paving the way for rigorous quantification of earthquake hazard.

Inside

Global Positioning System (GPS) Studies

2.1 Style of Deformation and Convergence Rates Across the Western Himalaya in Ladakh

Persistent collision of the Indian continent with Eurasia over the past 50 Ma, has created some of the most spectacular geomorphic features of the globe, notably the Himalaya, the Karakoram and the Tibetian plateau which together span a wide deformation zone more than 2,000 km across. Several studies over the past quarter century led to the recognition that a substantial part of the Indo-Eurasian convergence is absorbed by the overthrusting of India's fractured leading edge onto itself, a process that raised and sustains the mighty Himalaya, creating every few hundred years a series of great earthquakes from west to east. The remainder is used up in deforming the region north of the Himalaya where a series of east-west strike slip faults, of which the Karakoram and the Altyn Tagh are the most prominent, are regarded by some scientists to mediate strain relief, although the actual mechanism whereby this is effected has remained a matter of controversy. The second most prominent consequence of Indo-Eurasian convergence has been the thickening of the crust beneath Tibet and in the Tien Shan further north.

An understanding of the processes that have transferred several hundred kms of shortened crust to the thickened volume of Tibet thus remains an outstanding, yet unresolved issue. Two broad classes of models have been proposed to explain the doubling of the Tibetan crust in the light of physical evidence available and the understanding of physical principles. The first of these envisages that the Indian crust slides smoothly under Tibet involving little horizontal shortening of the latter. The second class of models, rooted in the image of the solid Indian plate as an indentor into the belly of Asia, are distinguished by the emphasis that is placed on the first or the second of the following two propositions after analyzing, landsat imageries from Asia: that i) the deformation of Asia appeared to be in some way dominated by strike slip faults suggesting lateral transfer of intervening materials eastwards out of the way of India's advance, and ii) that Asia, and perhaps, continents generally, behaved like a plastic deformable medium, and not like a stack of a few rigid plates. The indentor models whose implications are more in accord with the major large scale features of the collision zone, are today the most widely accepted. However, differing views of the estimates of the slip rates on the major strike slip faults of Asia, have led to their divergence into two extreme views of continental tectonics.

Motivated by the desirability to narrow these uncertainties, a GPS Geodesy Experiment was designed to constrain the kinematics of north-western trans-Himalaya, including slip rates on the Karakoram fault in Ladakh, generally regarded as one of the earth's greatest strike slip faults and most consequential in controlling the kinematics of southern Asia. In particular, GPS experiment was designed to define with a focus on estimating the following quantities: i) internal deformation of Ladakh in the nothwestern trans-Himalaya including the part of strain associated with the slip on the Karakoram fault, ii) rate of slip along the Karakoram fault using GPS as precisely dated offset landforms using cosmic ray exposure ages, since restriction of GPS control points to Indian territory i.e., to the southwest of the fault would reduce the slip rate signal to half, iii) rate and style of convergence across this segment of the Himalaya, iv) test of the east-west extension of the Tibetan plateau.

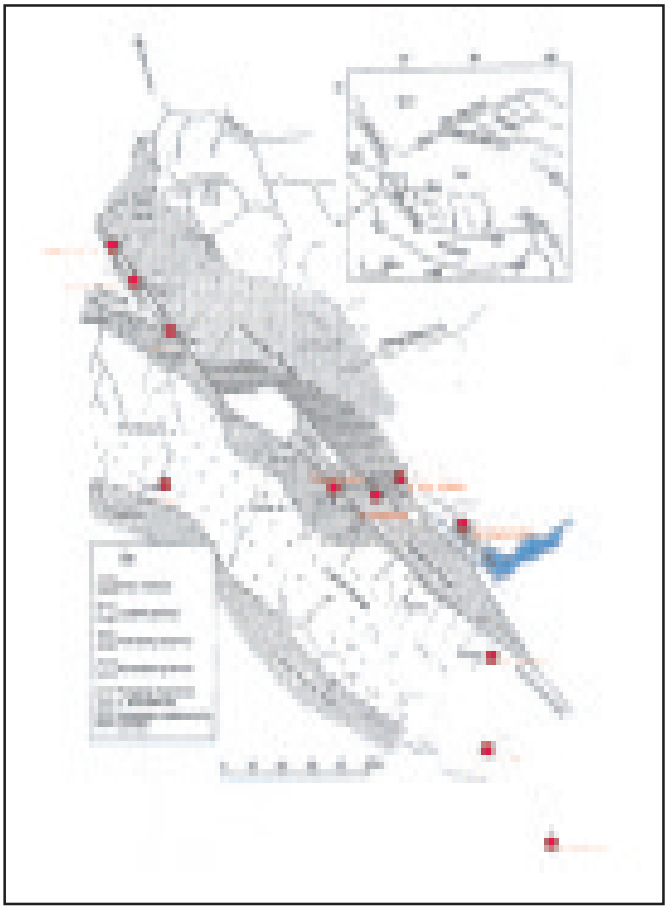

Fig. 2.1 C-MMACS GPS points superposed on geological map of Karakoram fault in northen Ladakh.

Two long running (Delhi and Leh) and eight campaign GPS control points (Fig.2.1) were installed in Ladakh in 1997 and 1998 to address the scientific goals stated above. Leh is situated about 60 km south west of the Karakoram fault, far enough to realistically record the elastic strain rate. All other sites incuding Chushul, the farthest east, were situated within 10 km of the surface trace of the Karakoram fault. The velocities of these sites relative to Leh is therefore expected to show only half or less of the slip rate on the fault. Analysis of GPS data generated at some of these sites between 1997 - 2000, and at most, between 1998-2000, in several different reference frames, yielded the following results: In the regional reference frame, relative velocities of all Ladakh sites (Fig.2.2) with respect to Leh is significantly nonzero only for Chushul which moves at 4.3±2.9 mm/yr at N142*E with respect to Leh, giving perhaps, a lower bound for the slip along the Karakoram fault.The velocity of Delhi (Fig.2.2) with respect to Leh is 16±2 mm/yr at N48*E. This represents the convergence rate across the Himalaya in the northwest. It is slightly less than, but indistinguishable from, the 18±2 mm/yr reported for Nepal and Kumaon. Furthermore, the direction corresponds to convergence normal to the Himalayan arc at the longitude of Delhi. This result thus confirms that Tibet deforms radially all along its southern boundary, advancing over the Indian continent more like a fluid body. Also implied is the corollary that the main accomodation of Indo-Eurasian convergence takes place i) across the Himalaya and ii) across the Tien Shan as the annual convergence across the latter together with this figure for the Himalaya will sum up to the total velocity of the Indian plate with respect to Eurasia. All Ladakh sites move at about the same rate, relative to Lhasa, at 13.2± mm/yr at N100*W, nearly due west (Fig.2.2).

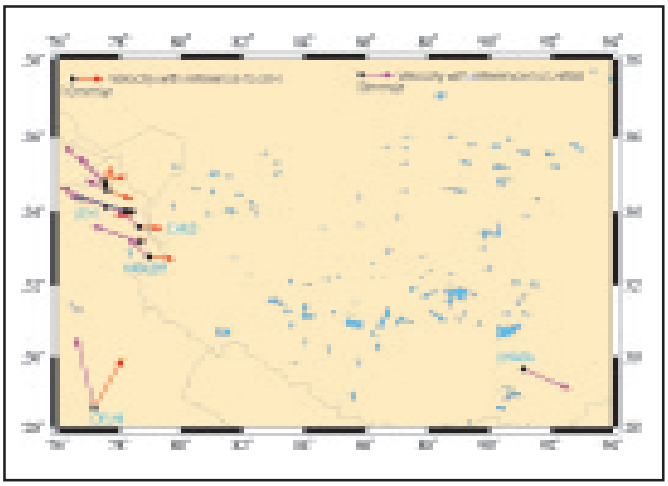

Fig. 2.2 Motion of Ladakh GPS points, Lhasa (IGS station) and Delhi in Leh fixed and Lhasa fixed reference frame.

This figure represents the rate of east-west stretching of Tibet, in agreement with previous estimates based on a shorter baseline between Lhasa and Simikot. The slip rate on the Karakoram fault inferred by us using GPS Geodesy and cosmic ray exposure ages of an offset debris flow in Ladakh, are ~ 4 mm/yr. An important implication of this result is that the Karakoram fault whilst remaining an important feature of the Indo-Eurasian convergence zone, cannot play a major role in accomodating this convergence in some plate tectonic fashion.

The north-south convergence is mainly accomodated by crustal thickness and that the outward (eastward extrusion) movement of the boundary can not be greater than about one fourth of the convergence rate in the collision zone. It thus appears most likely that Tibet does not behave as a rigid body and that plate tectonics, sensu stricto, ought not be applied to Tibet.

(Sridevi Jade, B C Bhat, M B Anand, P Dileep Kumar, and V K Gaur) * IAA, Leh*

2.2 Estimates of Coseismic Displacement and Post-Seismic Deformation

An earthquake of Moment magnitude M_w = 7.6, rocked the Rann of Kachchh and adjoining areas at 8 hours 46 minutes (IST) on the morning of January 26, 2001 (Fig. 2.3). This is the second catastrophic earthquake to have occurred in Kachchh, 181 years after the M 7.5 earthquake of June 1819 which destroyed the towns of Bhuj and Anjar and created an 80 km long fault scarp and a natural dam (Allah Bund) uplifted at its crest by 6.5 metres, on the northern edge of the Rann of Kachchh. The death toll of this earthquake already exceeds 10 times that of the 1819 event because of increased population making it the most lethal of Indian earthquakes so far. The earthquake affected a large area with a heavy toll of life (Officially 20005) and property estimated at Rs. 21262 million (www.ndmindia.nic.in/eq2001/sit.html).

Palaeoseismic indicators reveal that severe earthquakes have repeatedly occurred in this region over the past thousand years; the oldest evidence pointed to an earthquake inferred to have occurred 800-1000 years ago. The two major Kachchh earthquakes of 1819 and 2001 also happen to be the two largest historical events to have occurred anywhere within the continent. The 1819 event was the first major intra-continental earthquake for which crustal deformation was quantified; the earthquake was inferred to have occurred along a steep 80 km long NNW-SSE reverse fault dipping at 55± 5° N with slip of

11± 2metres. The epicentre of the 2001 earthquake lies about 70 km SSE of that of the 1819 event.

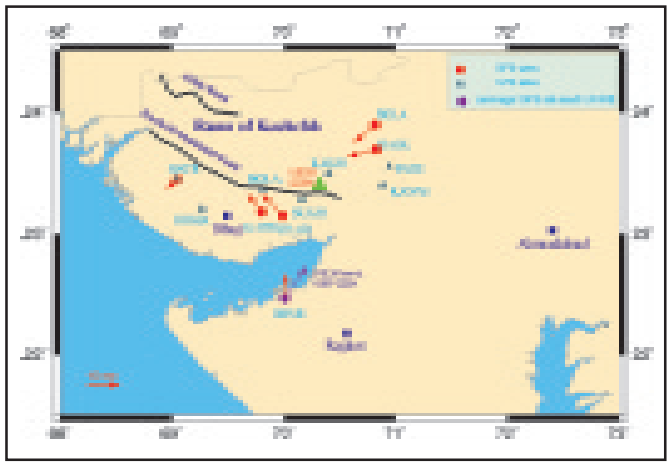

Fig. 2.3 Coseismic and post-seismic displacement vectors at the GPS sites of Bhuj GPS campaign.

The history of the Kachchh Rift Basin (KRB), the site of the Bhuj 2001 earthquake, began at about 150 Ma with initial opening of the Kachchh rift and continued to widen. During all this time the Kachchh Rift Basin was subjected to extensional stresses and inversion from extensional to compressional tectonics occurred around 20 Ma by which the basin was subjected to NNE-SSW directed compression. North dipping Kathiawar fault and south dipping Nagar Parkar Fault are extensional faults that form the southern and northern boundaries of the KRB respectively. The NNE-SSW compression has resulted in the formation of two systems of thrust faults within the KRB. The northern Allah Bundh system of thrust faults are NNE dipping with transport direction from NNE to SSW whereas the southern Kachchh Mainland Fault system of thrust faults dip to the SSW and have SSW to NNE transport direction. The zone of transition between the two systems of thrust faults lies almost entirely in the Great Rann. The entire KRB has been seismically active; the 1819 earthquake occurred in the northern system of faults whereas the 1956 Anjar and the 2001 Bhuj earthquake occurred in the southern system of thrust faults. The Bhuj 2001 earthquake was initially thought to have originated on the Kachchh Mainland Fault (e. g.); subsequent analysis of aftershocks and geology have indicated that the hypocentre of the 2001 earthquake was located in the footwall of the Kachchh Mainland Fault probably along a blind thrust dipping 40°-50° S and trending ENE-WSW and parallel to the Kachchh Mainland Fault.

Several teleseismic interpretations of the Bhuj earthquake have been proposed based on waveform modelling. These embrace a range of rupture areas, epicentral locations and slip vectors. Geodetic measurements in the epicentral region offer an alternative and potentially less ambiguous interpretation of the rupture parameters of the recent earthquake. Keeping this in mind, C-MMACS launched a GPS Campaign in the KRB to estimate coseismic displacements as well as post-seismic viscoelastic deformation expected to reflect the visco-elastic relaxation.

Global Positioning System (GPS) measurements (Fig.2.3) were made at 7 Great Triangulation Survey (1859) points along with the 5 GPS points (Hathria, Charakda, Khatrod, Bela and Dajka) established by C-MMACS in the epicentral area of the Bhuj earthquake and at Jamnagar south of the KRB to estimate the total residual displacements at these sites as a result of the 2001 Bhuj earthquake. The Jamnagar site was measured earlier in 1997 while the 7 GTS sites had been established during the GTS 144 years ago. Comparison of GPS (1997)-GPS (2001) coordinates at Jamnagar give the coseismic displacement vector(Fig.2.3)of 16±8 mm at N35^{o}E for the four year period (1997-2001); this is the only GPS-GPS based estimate of coseismic slip of the Bhuj 2001 earthquake. This displacement at Jamnagar is consistent with elastic models of the Bhuj earthquake (using slip parameters estimated from teleseismic data) that indicate that displacements of 2-5 cm may have occurred at this. This suggests that preseismic strain rates applied to the Kachchh region were not excessive compared to those prevailing in central India. The uncertainties observed with all the seven GTS sites reoccupied after the Bhuj 2001 earthquake indicates that computation of GTS-GPS displacement vectors is best avoided and only GTS-GPS baseline lengths between stations should be compared. Comparison of GTS (1857) and GPS (2001) baselines (Fig. 2.4) along and across the NNE-SSW compression or transport direction reveals shortening of 2.204 x 10 $^{-6}$ and elongation of 4.0436 x 10 $^{-5}$ respectively. This result indicates that the GTS (1857)-GPS (2001) baselines oriented at low angles to the NNE-SSW compression or transport direction have shortened in length while those oriented at high angles have been elongated. The two epochs of measurements at the 5 GPS sites in KRB and Jamnagar during the months of February and July, 2001 yield post seismic displacement rates (Fig. 2.3) averaging about 1mm/month at these sites. The post-seismic displacement vectors at the 5 GPS sites in the KRB and Jamnagar indicate that the displacement related to the post-seismic rheological reworking of the lower crust is superposed on the deformation related to the thrusting in the KRB. All the GPS baselines (Fig. 2.4), irrespective of

their azimuth, have shortened; the magnitude of shortening is highest along the Charakda-Khatrod baseline (shortening of 1.2873×10^{-7} at strain rate of 3.09×10^{-7}/year) and lowest for the Hathria-Bela baseline (shortening of 0.909674×10^{-8} at strain rate of 0.218321×10^{-7}/year).

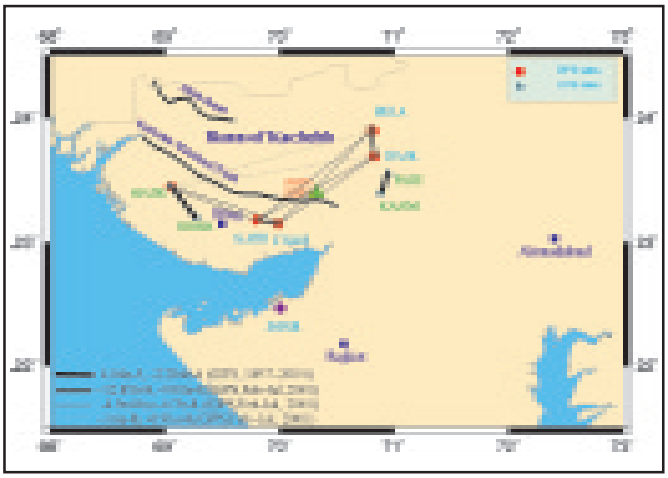

Fig. 2.4 Elongation (+) and shortening (-) of the GTS/GPS baselines.

Given that the azimuth of the Charakda-Khatrod baseline is 98.98° and that of the Hathria-Bela baseline is 76.02° (Fig.2.1), the latter is closer to the regional NNE-SSW compression direction and hence should be exhibiting maximum shortening rather than the minimum. However, the Hathria-Bela baseline is farthest from the epicentre and the Charakda-Khatrod line the closest. This indicates that the minimum and maximum shortening of the Hathria-Bela and Charakda-Khatrod baselines are directly related to their distance from the epicentre and, therefore, is probably controlled by post-seismic deformation rather than the NNE-SSW regional compression.

(Sridevi Jade, Malay Mukul, Imtiyaz A Parvez, M B Ananda, P Dileep Kumar and V K Gaur)

Earthquake Hazard Analysis

2.3. Attenuation of Strong Ground Motion Amplitudes in the Himalayas

The Himalayan region in India is one of the most seismically active areas of the world. The region forms the collision plate boundary between the Indian and Eurasian plates and has experienced many great earthquakes (M>8) that have inflicted heavy casualties and economic damages. Hence, it is essential to assess the intensities of severe ground motion in order to specify appropriate structural design loads and to undertake other countermeasures. The determination of ground motion relationships describing peak ground acceleration and velocity as a function of magnitude and hypocentral distance constitute the fundamental quantities required for the quantitative assessment of earthquake hazard and represent an important step in solving this problem.

Since the installation of three limited-aperture strong- motion networks in the Himalayan region in 1986 (Fig.2.5), seven earthquakes with M_w=5.2-7.2 have been recorded up to 1999. The data set of horizontal peak accelerations and velocities consists of 202 -component data for the hypocentral distance range of 10-400 km. This data set is limited in volume and coverage and, worst of all, it is highly inhomogeneous. Thus, we could not determine regional trends for amplitudes by means of the traditional approach of empirical multiple regression. Instead, we perform the reduction of the observations to a fixed distance and magnitude using independently defined distance and magnitude trends. To determine an appropriate magnitude-dependent distance attenuation law, we use the spectral energy propagation/ random function approach and adjust its parameters based on the residual variance. In doing so, we confirm the known, rather gradual mode of decay of amplitudes with distance in the Himalayas and it seems to be caused by the combination of high Qs and crustal wave-guide effects for high frequencies.

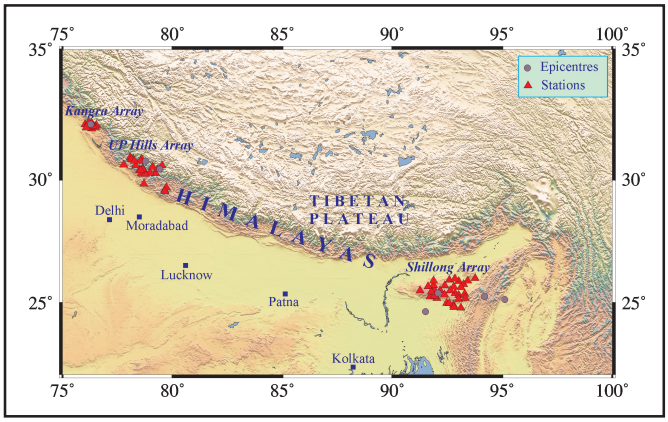

Fig. 2.5 Generalized geological and topographical map along with the strong-motion arrays and location of the events in Himalayas recorded by the network.

The data are then reduced with respect to magnitude. For the resulting set of reduced $\log_{10}$(peak acceleration) data, the residual variance is 0.37^2, much above commonly found values. However, dividing the data into two geographical groups, Western Himalayas (WH) with 3 events and Eastern Himalayas (EH) with 4 events, reduces the residual variance to a more usual level of 0.27^2 (station/site component of 0.22^2 and event component of 0.16^2). This kind of data description is considered acceptable. A similar analysis is performed with velocity data, and

again we have to split the data into two sub-regional groups. With our theoretically grounded attenuation laws, we attempt a tentative extrapolation of our results to small distances and large magnitudes.

In Fig.2.6(a), we represent our results as two families of peak acceleration $A_{max}(r)$ curves for a set of M_w values. The red curves are our predicted values for the EH and the green ones represent the trend for WH. Each event of our very modest database is represented by its centroid (dot) and by a segment describing the data ranges in orange colour for EH and in light blue for WH. The minimum estimates of peak acceleration for the epicentral zone of M_w=7.5-8.5 events is A_{max} = 0.25-0.4 g for WH, and as large as A_{max}=1-1.6 g for EH. In Fig.2.6(b), we compare our results on expected A_{max} vs. hypocentral distance to the results obtained by other researchers, for fixed M_w=7 (or M_L=6.7). The thick red line represents our results for EH and the thick green line for WH. One can see from this figure that our result for EH is unusually high as compared to all the others except that of Chandrasekaran, whereas our results for WH are quite comparable to others. The closest analog of our EH result, both in terms of level and shape of attenuation curve, is the trend of the eastern United States given by Atkinson and Boore.

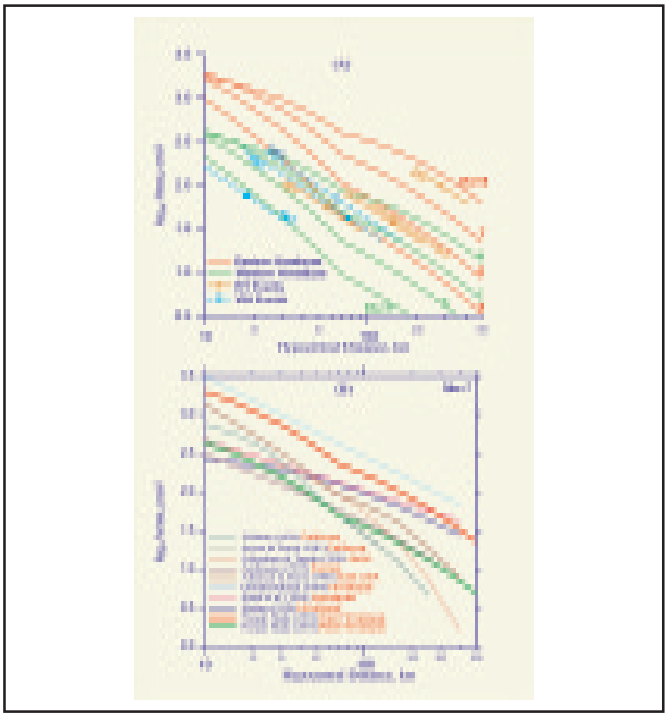

Fig. 2.6 (a) Attenuation laws of Log_{10} peak acceleration for small distances and large magnitude. The red curves are the predicted values for the EH and the green ones are for the WH. The orange and light blue lines are the segments of the observed data with their centroid for EH and WH respectively. (b) Comparison of our attenuation laws with those of other authors. Our results are represented by the thick red line for the EH and thick green line for the WH for M_w=7. The thin curves with different colors are given by different authors for different regions of the world.

Similarly, the established semi-empirical relationships of peak velocity V_{max} with hypocentral distance for EH in red colour and for WH in green colour are represented in Figure 2.7(a) for M_w=5, 6, 7 and 8. The expected minimum epicentral values of V_{max} for M_w=8 are 35 cm/s for Western and 112 cm/s for Eastern Himalayas. Each event of the database is also represented by its centroid and by a segment describing the data range in orange and lightblue colour for EH and WH regions. Fig.2.7(b) shows the comparison of our expected V_{max} versus hypocentral distance relationship with published trend of other regions. We see again that our result for EH is unusually high, above all the others at distances in excess of 50 km, whereas our results for the WH look quite regular. To understand whether our results reflect the properties of the subregions and not of a small data set, we check them against macroseismic intensity data for the same subregion. The presence of unusually high levels of epicentral amplitudes for the eastern subregion agrees well with the macroseismic evidence, like the epicentral intensity levels of X-XII for the Great Assam earthquake of 1897.

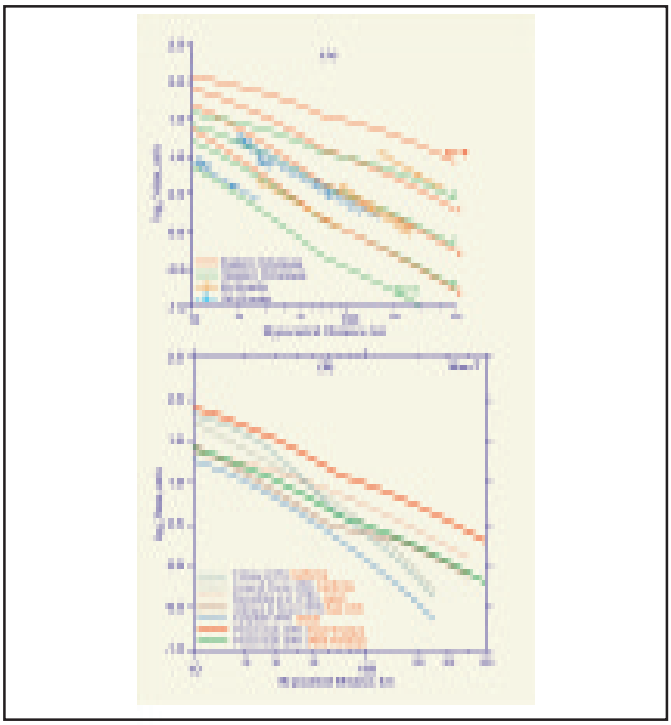

Fig. 2.7(a) Same as figure 2.6(a) but for log_{10} peak velocity. (b) Comparison of our results with those of other authors. Our results are represented by the thick red line for the EH and the thick green line for the WH for M_w=7. The thin curves with different colors are given by different authors for different regions of the world.

Therefore, our results represent systematic regional effects, and they may be considered as a basis for future regionalized seismic hazard assessment in the Himalayan region. As the main cause of the observed enhanced amplitudes for the Eastern Himalayas events, we see the location of earthquake sources/faults at a considerable depth within the relatively dryer and higher-strength shield crust. Western Himalayas sources are at lesser depth and occupy the tectonically highly fractured upper part of the crust, of accretionary origin. The low attenuation common to both subregions is due to the presence of cold, low scattering and high-Q shield crust.

(Imtiyaz A Parvez, A A Gusev and G F Panza**)*
** Institute of Volcanic Geology and Geochemestry, Russion Academy of Sciences, Kamchatsky, Russia.*
***The Abdus Salam International Centre for Theoroetical Physics, Trieste, Italy.*

2.4. A Deterministic Seismic Hazard Map of India and Adjacent Areas

The Indian subcontinent is one of the most earthquake prone areas of the world. The main seismogenic zones are associated with the collision plate boundary between the Indian and Eurasian plates and is marked by the Kirthar Sulaiman, Himalayas and Arakan-Yoma mountain ranges. Eleven great earthquakes of magnitude 8.0 and above have occurred in this subcontinent during the last two centuries, which clearly indicates the tectonic and structural trends along the collision plate boundary. These devastating earthquakes inflicted heavy casualties and economic damages to the country and the neighbouring areas. One way to mitigate the destructive impact of the earthquakes is to conduct a seismic hazard analysis and take the remedial measures.

A seismic hazard map of the territory of India and adjacent areas has been prepared using a deterministic approach based on the computation of synthetic seismograms complete of all main phases. The input data set consists of structural models, seismogenic zones, focal mechanisms and earthquake catalogue. The synthetic seismograms have been generated by the modal summation technique. The seismic hazard, expressed in terms of maximum displacement (DMAX), maximum velocity (VMAX), and design ground acceleration (DGA), has been extracted from the synthetic signals and mapped on a regular grid of 0.2° x 0.2° over the studied territory. The estimated values of the peak ground acceleration are compared with the observed data available for the Himalayan region and found in good agreement.

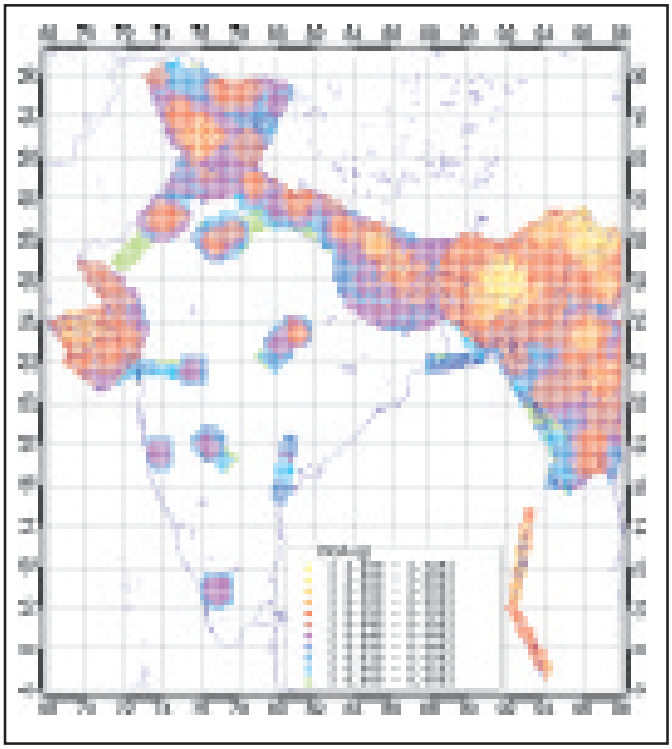

Fig. 2.8 Spatial distribution of the design ground acceleration (DGA) in g.

Fig.2.8 shows the Design ground Acceleration (DGA) map of the Indian Subcontinent. The maximum values of DGA have been estimated over the north East Indian region in the epicentral zone of the great Assam earthquakes of 1897 and 1950. The DGA values obtained for this region are ranging between 1.0 to 1.3 g. The Bihar-Nepal and Central Himalayan region have the DGA values between 0.3 and 0.6 g. In part of western Uttar Pradesh and in the epicentral zone of Uttarkashi earthquake of 1991 the estimated DGA values are between 0.15 to 0.3 g. In many parts of the epicentral zone of Kangra and Kutch earthquakes and in some parts of the Andaman and Nicobar islands the DGA reaches up to 0.6 g. The three metropolitan and biggest cities of India, with relevant industrial and economical importance, namely Delhi, Mumbai and Kolkata lie in the hazardous zones of the DGA map. The most severe hazard is in Delhi and its surroundings where DGA estimate is as high as 0.3 g, while in the other three big cities still DGA estimates are below 0.1 g. The DGA estimates in Peninsular India are less than 0.15 g, and only in the Latur region DGA values close to this upper limit are obtained. Fig.2.9 shows the peak velocities mapped over the entire territory. The highest peak velocities are obtained again in the Northeast India as 120-170 cm/sec. In the other parts of the region, like central and western Himalayas, western Uttar Pradesh, Himachal Pradesh and some parts of the Gujarat State, maximum velocity is up to 120 cm/sec. In

the area of Andaman and Nicobar the maximum velocity is in the range 60-120 cm/sec.

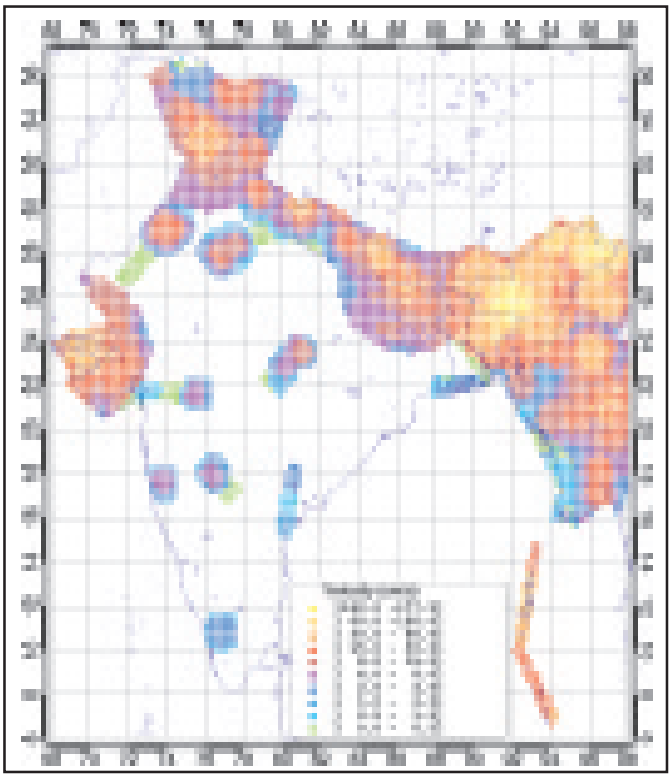

Fig. 2.9 Spatial distribution of the estimated peak ground velocity in cm/sec.

The deterministic modelling of hazard for the Indian territory provides us a powerful and economically valid scientific tool for seismic zonation and hazard assessment. The main advantage of the method lies in its ability to directly estimate the effects of source mechanics and wave propagation, while local site effects are roughly considered when using the design spectra to obtain the DGA from the synthetic response spectra. We believe that the data we present here will contribute to a better understanding of the seismic hazard in India and neighbouring areas. Furthermore, our multidisciplinary approach may help to those earthquake and civil engineers who wish to undertake comprehensive and detailed studies of earthquake hazard especially in Himalayan eastern region, eastern and western India and some big cities like Delhi, Mumbai and Kolkata.

(Imtiyaz A Parvez, F Vaccari and G F Panza*,**)*

** Department of Earth Sciences, University of Trieste, Italy*

*** The Abdus Salam International Centre for Theoretical Physics, Trieste, Italy.*

2.5. A Pilot Study for the Deterministic First Order Microzonation of Delhi City

The recent Bhuj earthquake of January 26, 2001 has left thousands dead, hundreds of thousands injured and a much large number destitute. Damage to property apparently runs into billion of Rupees. This was a shocking event that generated untold misery and captured media attention around the world. Although located about 300 km away from the epicentre of the earthquake, Ahmedabad, one of the largest cities in India, suffered severe damage due to this event. Several other megacities in India, such as Delhi, Mumbai, Kolkata and Guwahati etc., face severe earthquake hazard. A growing number of large industrial settlements are also located in earthquake-prone areas.

Delhi – the capital of India lies on a severe earthquake hazard threats not only from the local earthquakes but also from Himalayan events just 200-250 km apart. This is a fast growing megacity that influences the economic and industrial development of most of the country. The estimated population of urban Delhi is now around 12.5 million. An example of the study of site effects and microzonation of a part of metropolitan Delhi City is presented, based on a detailed ground motion modelling along two cross sections (Fig.2.10). The seismic ground motion is computed with a hybrid technique based on the

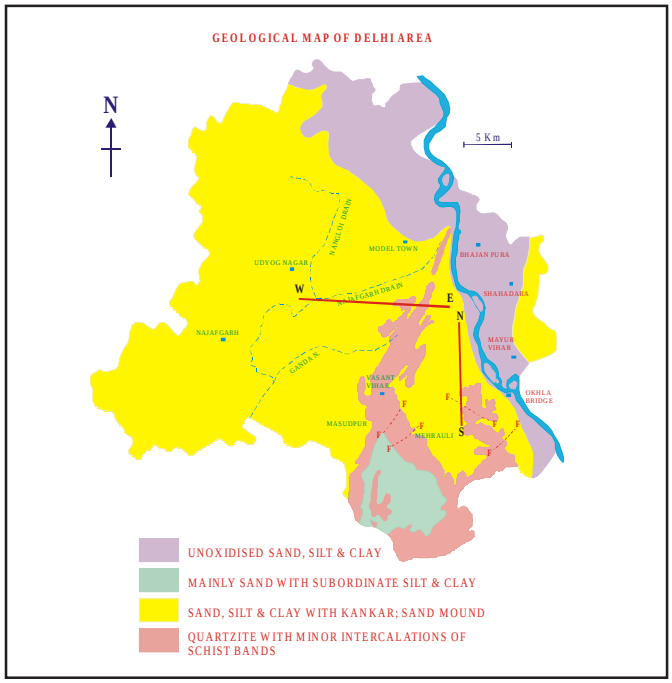

Fig 2.10 Generalized geological map of Delhi area and the locations of the cross-sections used in the present study for the numerical modelling.

modal summation and the finite difference scheme for site-specific strong ground motion modelling. Complete realistic SH and P-SV wave seismograms are computed along two geological cross-sections, (1) North-South, from Inter State Bus Terminal (ISBT) to Sewanagar and (2) East-West, from Tilak Bridge to Punjabi Bagh. Two real earthquake sources of July 15, 1720 (MMI=IX, M=7.4) and August 27, 1960 (M=6.0) have been used in modelling. The response spectra ratio (RSR), i.e. the response spectra computed from the signals synthesized along the laterally varying section normalized by the response spectra computed from the corresponding signals, synthesized for the bedrock reference regional model, have been determined. As expected, the sedimentary cover causes an increase of the signal amplitude particularly in the radial and transverse components.

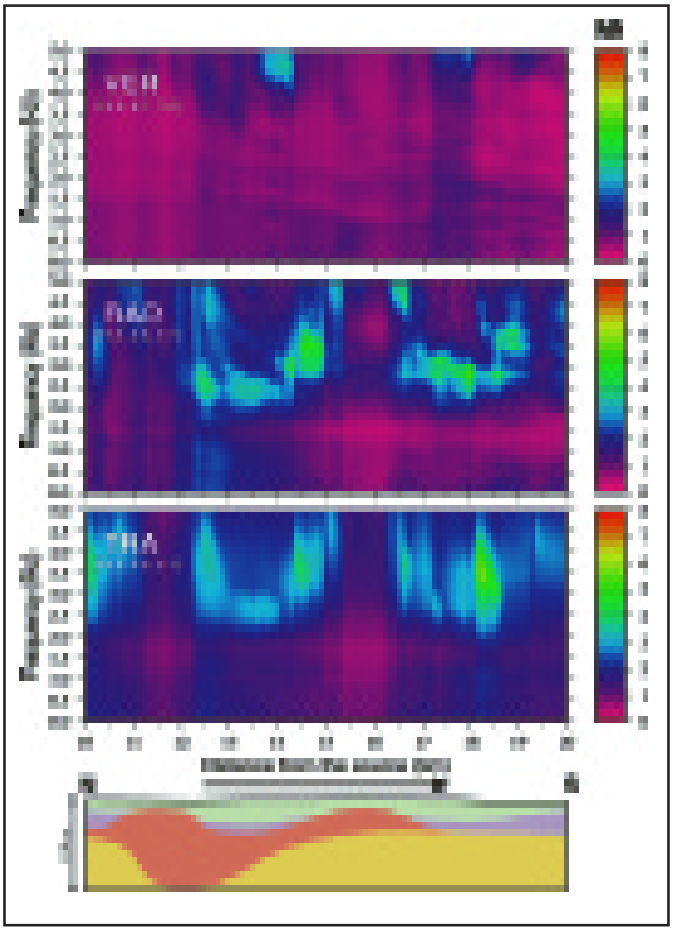

Fig 2.11 The NS cross-section and the corresponding plot of Response Spectra Ratio (RSR) versus frequency and distance. The numbers in brackets represent maximum amplification, in order, the distance in km, frequency in Hz and Value of the Peak RSR.

The distribution of RSR as a function of frequency and epicentral distance along the NS profile, up to a maximum frequency of 5 Hz is shown for the three components in

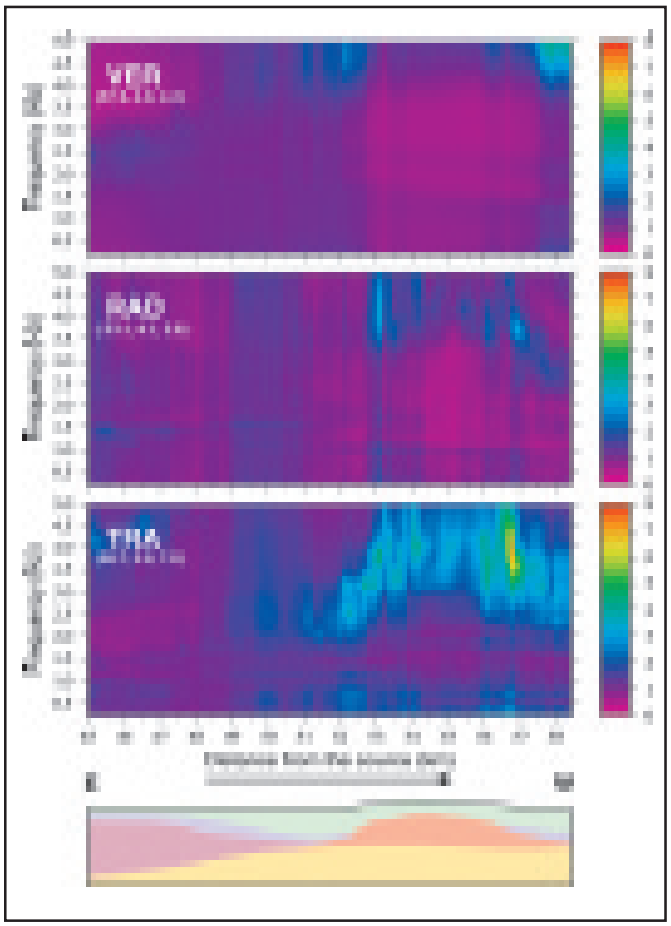

Fig 2.12 Same as figure 2.11 for EW cross-section.

Fig.2.11. For each component of motion, the numbers in parenthesis give the maximum amplification, in the order, the distance from the source in km, the frequency in Hz and the RSR value (amplification). A 5% damping of the response spectra is considered since reinforced concrete buildings are already or will be built in the area. There are sites, where the amplifications are relevant in all the three components, even if the maximum amplifications are always found in the horizontal components. The RSR ranges between 5 to 10 in the frequency range from 2.8 to 3.7 Hz, for the radial and transverse components of motion along the NS cross-section. The amplification of the vertical component is large at high frequency (> 4 Hz.) whereas it is negligible in lower frequency range. Fig.2.12 shows the similar results for EW cross-section. The maximum amplification is obtained in the transverse components, less than 8 at a frequency of 3.9 Hz, whereas in the radial component it is 3.6 at a frequency of 4.1 Hz.

Although this is a good starting point for the microzonation of Delhi, many more cross-sections will be required to cover the whole city, and an attempt is currently going on in such

a direction. One of the important aspects of the future study will be to model the site-effects, due to the sub-surface soil of Delhi City, as caused by an expected great earthquake in the Central Himalayas.

The vertical component shows the maximum amplification of 4.2, at much higher frequency of 4.9 Hz. The local amplifications, seen along the two profiles, tell us that, in general the local intensity (MCS) increments can be as large as two units, with respect to the average value, observed in the whole urban area. The results of this study can readily be applied to site-specific design spectra based on average or maximum amplification and should strictly be followed on revising the building codes. Such building codes must not only allow but encourage on demand the use of such site-specific design procedures on soft-soils, in order to protect buildings during earthquakes comparable to those we have considered in the modelling.

(Imtiyaz A Parvez, F Vaccari and G F Panza*,**)*

** Department of Earth Sciences, University of Trieste, Italy*
*** The Abdus Salam International Centre for Theoretical Physics, Trieste, Italy.*

Modeling Earthquake Dynamics

2.6 Contact Area Distribution Between Rough Surfaces

The role of the heterogeneity of the lithosphere in earthquake dynamics is not yet properly understood. One of the touchstones for any model that claims to mimic earthquake dynamics is the reproduction of Gutenberg-Richter (G-R) law between energy releases and slips- a power law. However, the simplest model for earthquake processes- the stick-slip dynamics approximated by the slider block model (the so-called Burridge-Knopoff model)- obtains a G-R law without incorporating any heterogeneities; uniform blocks connected by springs of uniform spring constants are enough to obtain a power law. In fact, the G-R law in this case is a result of the velocity weakening friction law in the model. The question regarding the role of the heterogeneities of the lithosphere in earthquake dynamics is, therefore, not resolved.

Efforts to incorporate heterogeneities (fractal structures, for example) in the standard slider-block models have also not identified the role of the heterogeneities in shaping the structure of earthquake data. In a basic model put out some time back, it was proposed that the contact area distribution between fractal surfaces follows a unique power law which was also conjectured to be applicable to the case of random surfaces. Simple arguments that employ a proportionality of the energy releases during slips with the contact areas lead to the conclusion that the G-R law can be arrived at from the power law relationship in overlap area distribution. While the above formalism is appealing, a numerical study carried out by us to investigate the nature of the contact area distribution shows that no power law is obtained for the contact area distribution between (identical) fractal/random surfaces. Instead, what is obtained is a quadratic (instead of a linear; for power laws) relationship in the log-log plot of the probability versus contact area (Fig. 2.13). We have shown this for a variety of different surfaces. It is clear that the model has to be re-examined in the light of these findings.

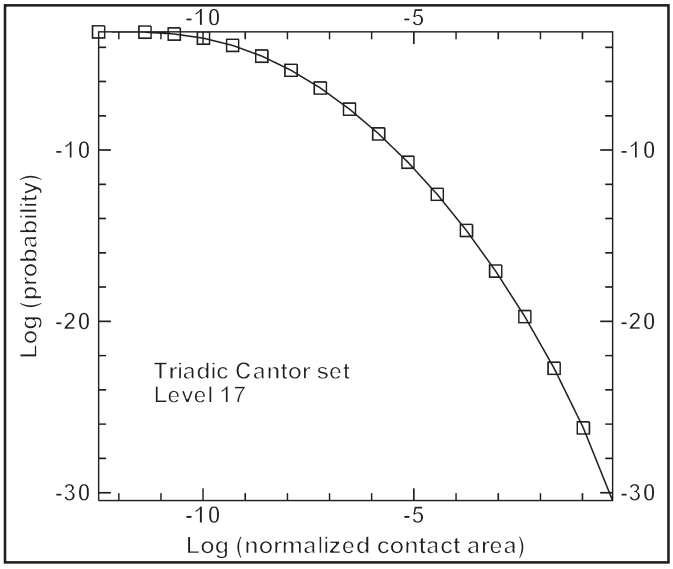

Fig 2.13 Probability versus normalized fraction of overlap area in a log-log plot.

It may be mentioned that the problem of contact area distribution is also of relevance in other contexts. One example is that of percolation inside fracture networks where the aperture and channel distributions have to be worked out. Also, in engineering, the accurate characterization of dry friction depends on the nature of contacts between the rough surfaces.

(T R Krishna Mohan)